Priddis low-frequency seismometer test, part 2

Kevin W. Hall, Gary F. Margrave, Malcolm B. Bertram, Dave W. Eaton

ABSTRACT

CREWES acquired a low-frequency sensor comparison test dataset in 2009. The dataset was acquired using a weight drop trailer and an IVI Minivibe (2-10 Hz and 2-100 Hz linear sweeps with different sweep lengths and peak force levels) at two source points, offset by 50 meters from the ends of the north-south receiver lines. Sensors on the ground included accelerometers (DSU3 and VectorSeis), geophones (SM-24) and broadband seismometers (Trillium 240). Near-offset (50 m) traces for a single 2-100 Hz linear sweep are visually compared as 1) uncorrected, uncorrelated data, 2) converted to common units and corrected for geophone and seismometer instrument response in the velocity and acceleration of ground motion domains. Quantitative least-squares-subtraction-scalar results are also presented. System electrical noise appears to dominate signal below about 7 Hz for all systems, likely due to the long taper used for the low frequencies (< 10 Hz) and the low power used for the sweep in order to not damage the Minivibe. We appear to have a close match (other than a multiplicative term) down to at least 5 Hz for all recording systems and sensors.

INTRODUCTION

CREWES acquired a low-frequency sensor comparison test dataset in 2009. The dataset was acquired using a weight drop trailer and an IVI Minivibe (2-10 Hz and 2-100 Hz linear sweeps at different sweep lengths and peak force levels) at two source points, offset by 50 meters from the ends of the north-south receiver lines. The sensors and recording systems used are listed in Table 1. The survey itself is described in greater detail by Bertram et al. (2009), Eaton et al. (2009), and Hall et al. (2009). Eaton et al. (2009) present some results comparing the geophone and seismometer data converted to strain for the weight drop source. Hall et al. (2009) introduced a least-squares-subtraction-scalar method for quantitatively comparing data from different sensors, and showed comparison results for the uncorrected, or raw, uncorrelated data geophone and accelerometer data recorded for all of the 2-10 Hz sweeps, compared to the calibrated seismometer data.

This report endeavours to 1) remove amplitude and phase effects due to instrument response from the raw geophone and seismometer data, 2) convert all data to velocity and acceleration of ground motion in units of m/s and m/s^2, and 3) compare the results visually and by least-squares-subtraction-scalars. The data used in this study are the vertical component, uncorrelated, near offset (50 m) trace for a single 2-100 Hz, 30 s linear sweep at the north source point (Aries and Trillium FFID 30, Sercel FFID 37, Scorpion FFID 169).

Table 1. List of recording systems, sensors, low-cut filters and sample rates.

Operator	Recording system	Sensor	Low-cut filter (Hz)	Sample rate (ms)
University of Calgary	ARAM/Aries	SM-24 geophone elements	1	2
ION	ION/Scorpion	VectorSeis	1.46	2
CGGVeritas	Sercel/428XL	DSU3	None	2
University of Calgary	Nanometrics/Taurus	Trillium 240 seismometer	0.004	10

DATA PREPARATION

Figure 1a shows the near-offset (50 m) traces for raw data recorded for a single 2-100 Hz sweep at the north VP for all sensors, the data are in a variety of units (Table 2). Note the orders of magnitude differences in the amplitude scales (from 10^{-2} to 10^6). Amplitudes on the Trillium trace, with a 50 Hz Nyquist frequency (see Table 1), die out about half-way along the 100 Hz sweep, as expected. To check if the sensitivities listed in Table 2 make sense, we convert to acceleration in units of m/s^2 by applying the sensitivities and differentiating the Trillium and Aries data (Figure 1b) using:

$$tra = \text{gradient}(Trillium/(1168.2*1e6), time),$$

$$ara = 0.5*\text{gradient}(Aries/20.5, time),$$

$$sca = 0.5*Scorpion*g \text{ and}$$

$$sea = Sercel/(408*1e4), \tag{1}$$

where Equation(s) 1 are the Matlab code used, *time* is a time vector, and *g* is assumed to be 9.81 m/s^2.

Table 2. Known parameters for the recording systems

System	Data Units	Sensitivity		Source
Trillium	μV	1168.2	V/m/s	Nanometrics (2008)
Aries	V	20.5	V/m/s at 0.7 damping	Hons (2008)
Scorpion	g			Vince Rodych (pers. comm.)
Sercel	mV	408	mV/m/s^2	Jim Roy (pers. comm.)

The Sercel data shown in Figure 1b are scaled by an additional 10^4, which could easily be due to a misunderstanding of the units on our part, (eg. g instead of Volts. Volts instead of milliVolts). Since we are taking the calibrated seismometer response to be the correct answer, the Aries and Scorpion data have been multiplied by one half, in order to better match the Trillium and Sercel amplitudes. This factor of two could possibly be due to a 6 dB difference in pre-amp gain in the recording systems (eg. Hons, 2008). Visually,

the resulting traces are quite similar, and the amplitudes are now of the same order of magnitude, giving us some confidence that our conversion to units of m/s² is likely correct. Equation 1 for the accelerometers is sufficient if the resonant frequency of the accelerometer (typically kHz; Hons, 2008) is sufficiently higher than the frequencies recorded. While accelerometer (micro-electromechanical systems, or MEMS, capacitance-force-balance-response system) response is flat to acceleration from zero to hundreds of Hertz (Hons, 2008), Equation(s) 1 do not account for instrument response in the geophone and seismometer data. The SM-24 geophone (resonant mass coil system) response is flat to velocity from 20-240 Hz, with a 3 dB down point at 10 Hz, the natural frequency of the geophone (SM-24 geophone element brochure, 2006). The seismometer (capacitance-force-balance system) response is flat to velocity from 240 s (0.004 Hz) to 35 Hz (Trillium 240 brochure, 2010).

The transfer function to convert the velocity of the geophone proof mass to the velocity of ground motion is given by

$$H = -S \frac{\omega^2}{-\omega^2 + 2j\lambda\omega\omega_0 + \omega_0^2}, \qquad (2)$$

where H is the frequency domain representation of the transfer function, S is the sensitivity, ω is the frequency, j is the square root of negative one, λ is the damping ratio and ω_0 is the natural frequency of the geophone (Hons, 2008). Equation 2 corrects for phase and amplitude effects that are present in the geophone data relative to ground velocity. The transfer functions for displacement and acceleration can be obtained by multiplying or dividing Equation 2 by $j\omega$, where $j\omega$ is equivalent to $\partial/\partial t$ in the time domain (Hons, 2008).

The transfer function for a seismometer (eg. Bogert, 1961) is given by

$$H = S \frac{\sum_{a=1}^{N} \omega - z_a}{\sum_{b=1}^{M} \omega - p_b}, \qquad (3)$$

where z_a and p_b are the complex zeros and poles of the transfer function. The nominal zeros and poles for the Trillium 240 are listed in the seismometer user manual (Eaton et al., 2009; Nanometrics, 2008). For the Trillium 240, the sensitivity (S) in Equation 3 is the sensitivity listed in Table 2 multiplied by a normalization factor of 4.517e5 rad² /s² (Nanometrics, 2008).

Figure 2 shows the results for the velocity of ground motion. In this case the accelerometer data has been multiplied by $j\omega$ in the frequency domain to integrate to velocity. Figure 3 shows the acceleration of ground motion, where equations 2 and 3 have been divided by $j\omega$ in the frequency domain to differentiate the geophone and seismometer data. The maximum amplitudes of the resulting curves are the same order of magnitude, and the curves look similar. The Trillium data are slightly different in detail, which can be attributed to the coarser sample rate. Figures 4-6 show the same data as Figures 1-3, but in the frequency domain. Note that the amplitude scale for these figures

is decibels (dB) relative to a reference amplitude of one, **not** decibels referenced to the maximum amplitude in each curve (dB down).

LEAST SQUARES SUBTRACTION SCALARS

Hall et al. (2009) introduced a frequency dependent least-squares-subtraction-scalar method, and showed results that were calculated in the time domain after filtering data with a sliding 1 Hz wide bandpass filter for the 2-10 Hz sweeps acquired in this survey. A least-squares-subtraction-scalar is the unique constant, a, that minimizes the sum-squared differenece between two traces S_1 and aS_2, where the second trace is being scaled. Two criticisms that resulted were 1) the mismatch in amplitudes in the raw data comparisons, and 2) the lack of correction for instrument response in the geophone and seismometer data. The least-squares-subtraction-scalar can be calculated by

$$a = \frac{\sum_k S_{1k} S_{2k}}{\sum_k S_{2k}^2}, \tag{4}$$

where S_{1k} and S_{2k} are the kth sample of traces S_1 and S_2. In general, if S_1 and S_2 are the same trace, a is equal to 1. For a phase difference of 90°, a is equal to zero, for a 180° phase difference, a is equal to -1. The order matters: if a equals 2, S_1 is twice the amplitude of S_2, if a equals 0.5, S_1 is half the amplitude of S_2. In a frequency-dependent sense (successively calculated a's for a sliding bandpass window), a horizontal line for a plotted versus frequency can be considered to be a perfect match between traces except for some multiplicative constant, if a is not equal to one.

Table 3 lists maximum amplitudes and least-square-subtraction-scalar results for raw data, data converted to velocity of ground motion, and data converted to acceleration of ground motion. For this table, the data used in Equation 4 are the frequency domain curves shown in Figures 4, 5 and 6 for a single 2-45 Hz window. This window was chosen because the low-end of the sweep was 2 Hz, and 45 Hz is below the large drop-off in Trilllium amplitudes due to the anti-alias filter for the corresponding 50 Hz Nyquist.

Figure 7 show the extension to frequency dependency, using 1 Hz wide sliding windows moving one sample per step in the frequency domain (1 sample = 0.167 Hz) from 0.5 to 45 Hz. The advantages of this approach are: 1) the Trillium data do not have to be interpolated from 10 ms to 2 ms, which may have introduced artifacts in the results of Hall et al. (2009), and 2) the traces do not have to be aligned in the time domain (there is no time-zero for Trillium, Sercel, or Scorpion data due to manual triggering of the recording instruments and/or continuous recording). Thus, total computation time is reduced, since the interpolation, trace alignment and filter steps reported by Hall et al. (2009) are replaced by a simple truncation in the frequency domain. This also allows reliable extension of the method to frequencies below 2 Hz. Figure 7 shows least-squares-subtraction results for the Fourier amplitude spectrum, and thus contains no information about frequency-dependent phase differences. The method could also be applied to the phase spectra (not shown).
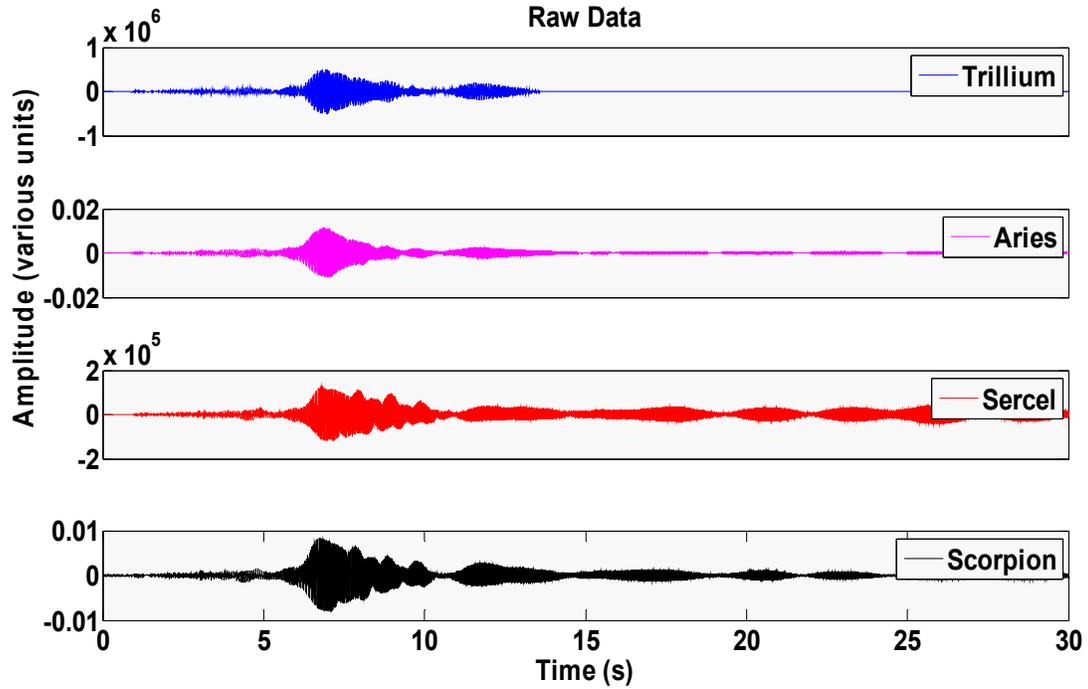
FIG. 1a. Visual comparison of vertical component, uncorrected uncorrelated data for a 30 s 2-100 Hz linear sweep for a 50 m source-receiver offset (north VP).
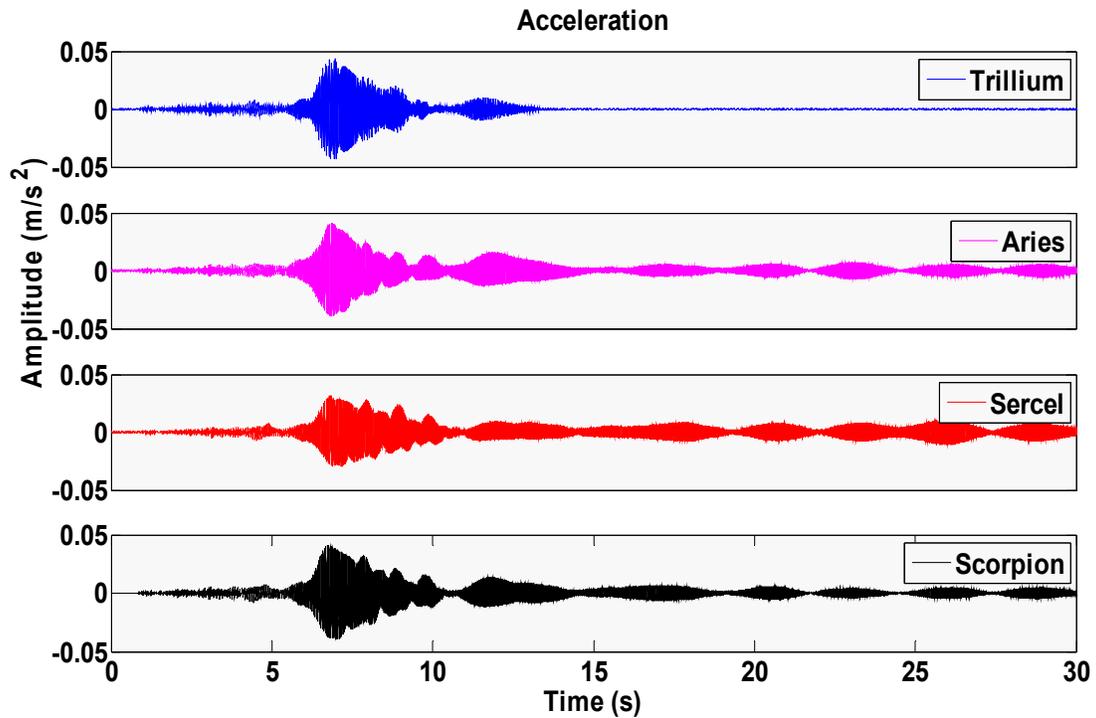

FIG. 1b. Visual comparison after converting raw data to acceleration with no correction for geophone or seismometer instrument response.
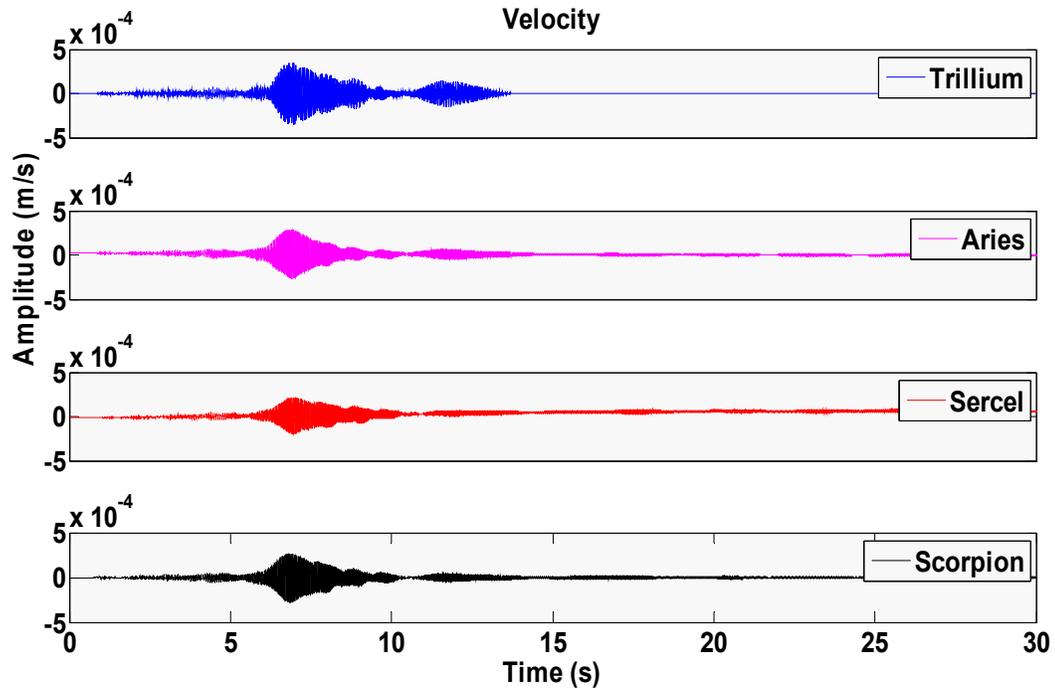
FIG. 2a. Visual comparison after converting raw data to velocity: data corrected for geophone and seismometer instrument response.
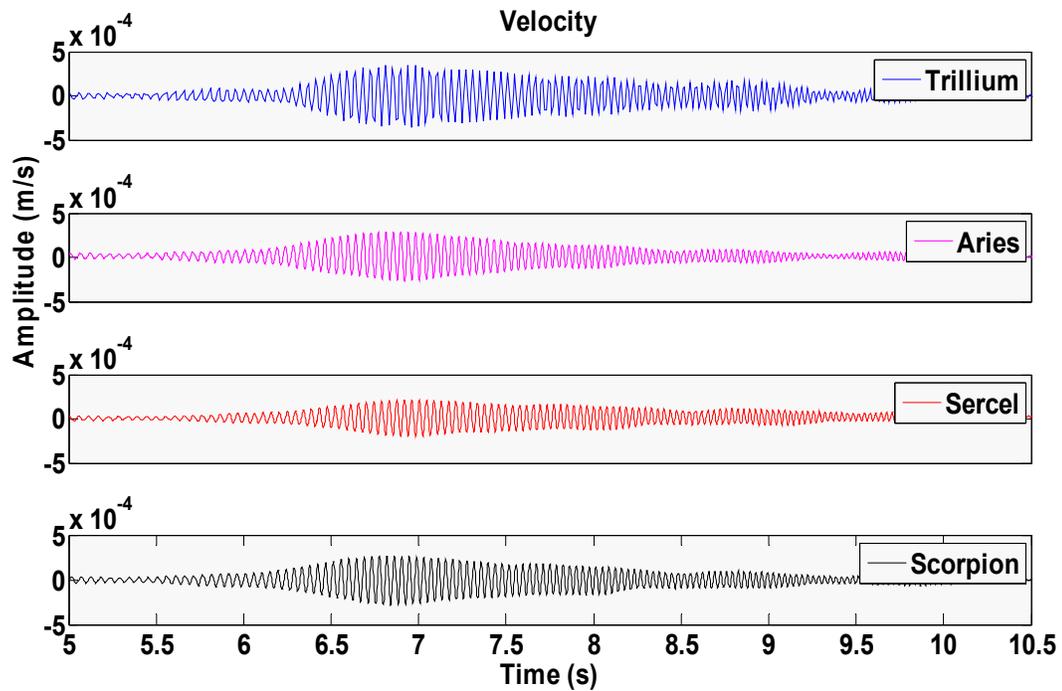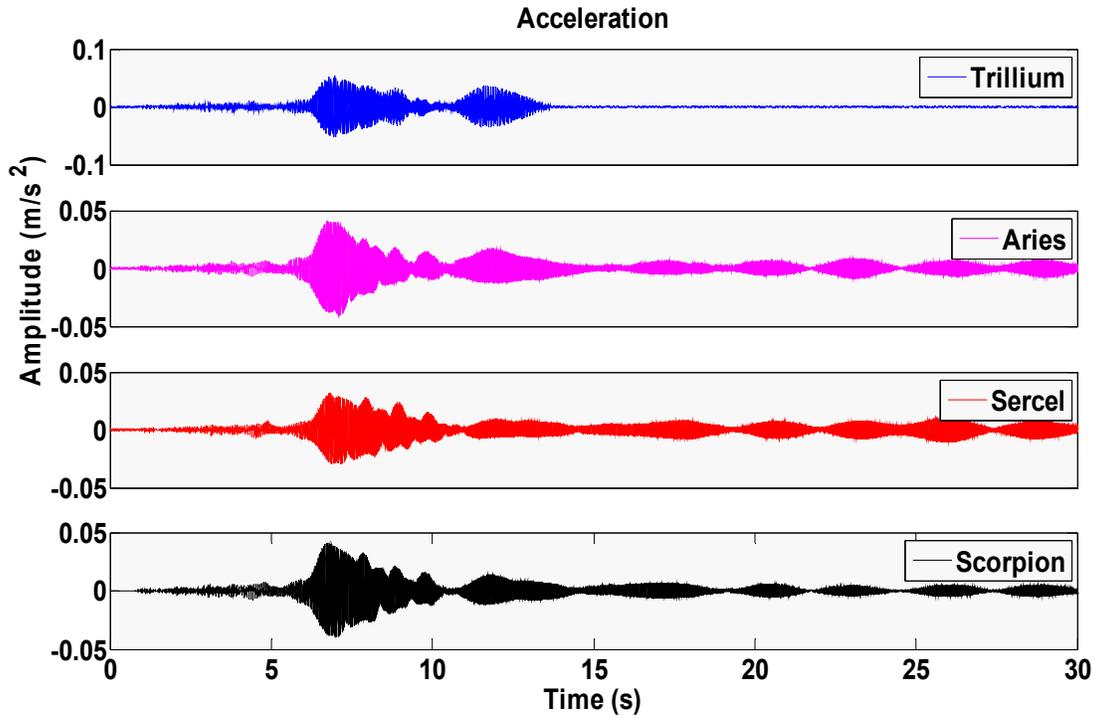

FIG. 2b. Visual comparison after converting raw data to velocity: data corrected for geophone and seismometer instrument response. (magnified portion of Figure 2a).

FIG. 3a. Visual comparison after converting raw data to acceleration: data corrected for geophone and seismometer instrument response (cf. Figure 1b).
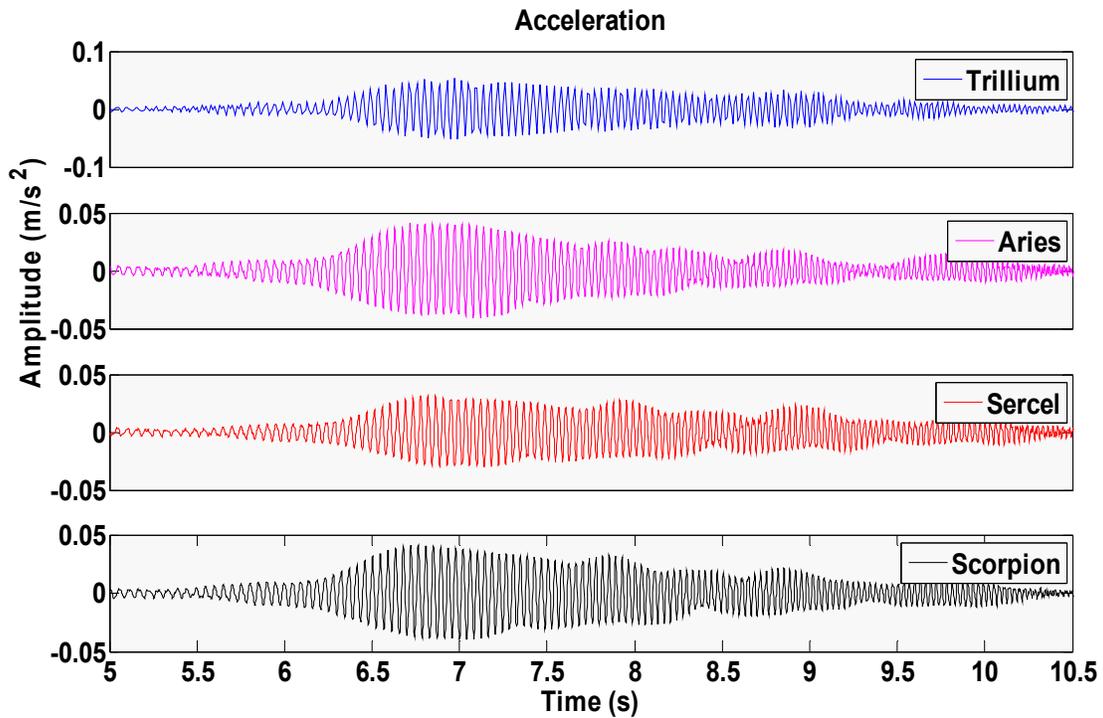

FIG. 3b. Visual comparison after converting raw data to acceleration: data corrected for geophone and seismometer instrument response. (magnified portion of Figure 3a).
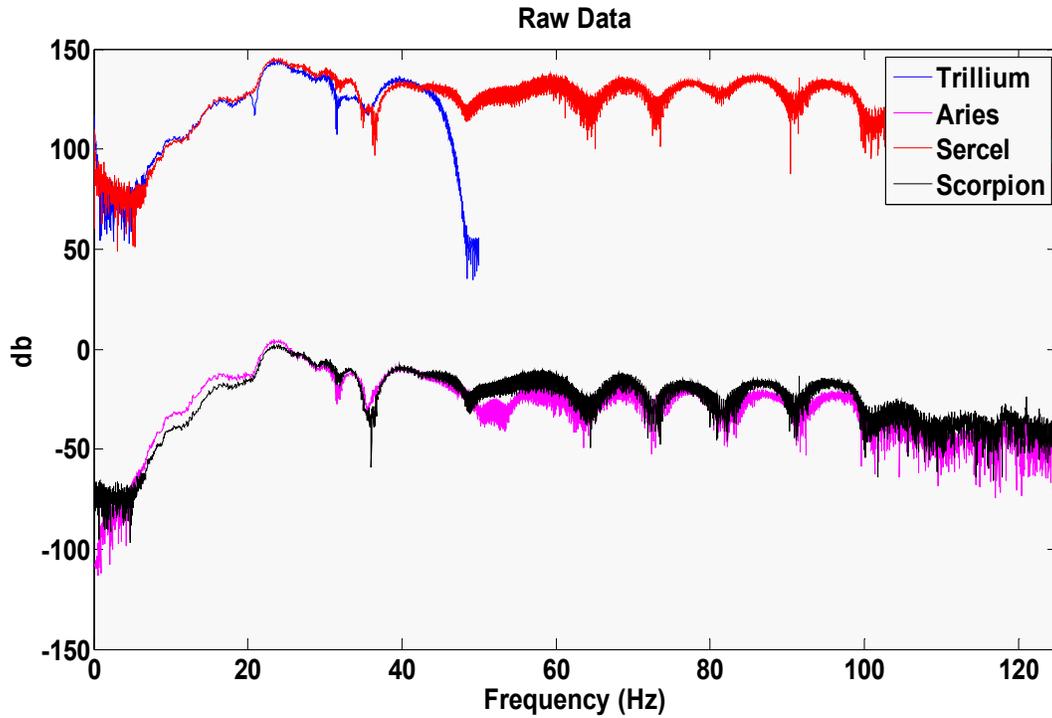
FIG. 4a. Visual comparison of vertical component, uncorrected uncorrelated data for a 30 s 2-100 Hz linear sweep for a 50 m source-receiver offset (north VP).
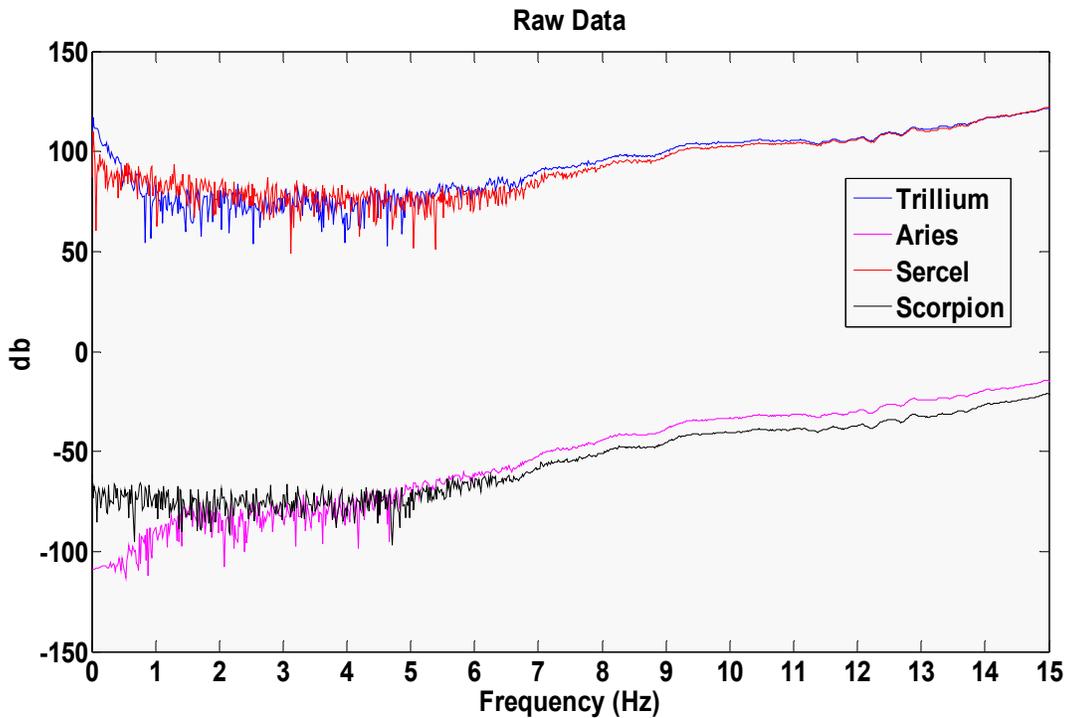

FIG. 4b. Visual comparison of vertical component, uncorrected uncorrelated data for a 30 s 2-100 Hz linear sweep for a 50 m source-receiver offset (magnified portion of Figure 4a).
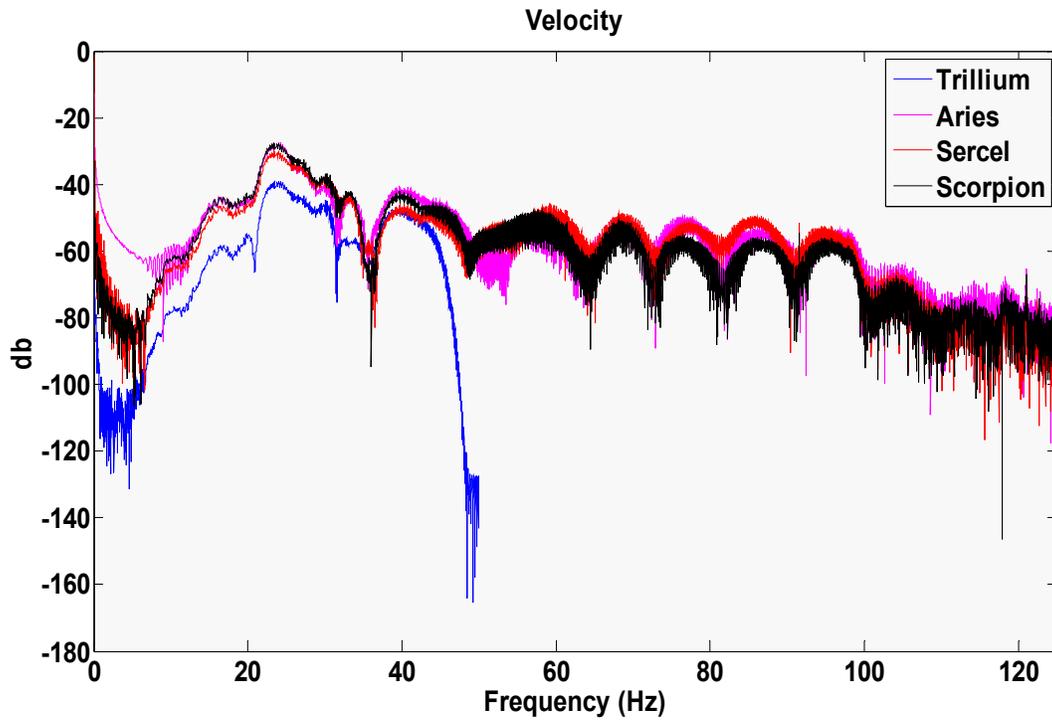
FIG. 5a. Visual comparison after converting raw data to velocity: data corrected for geophone and seismometer instrument response.
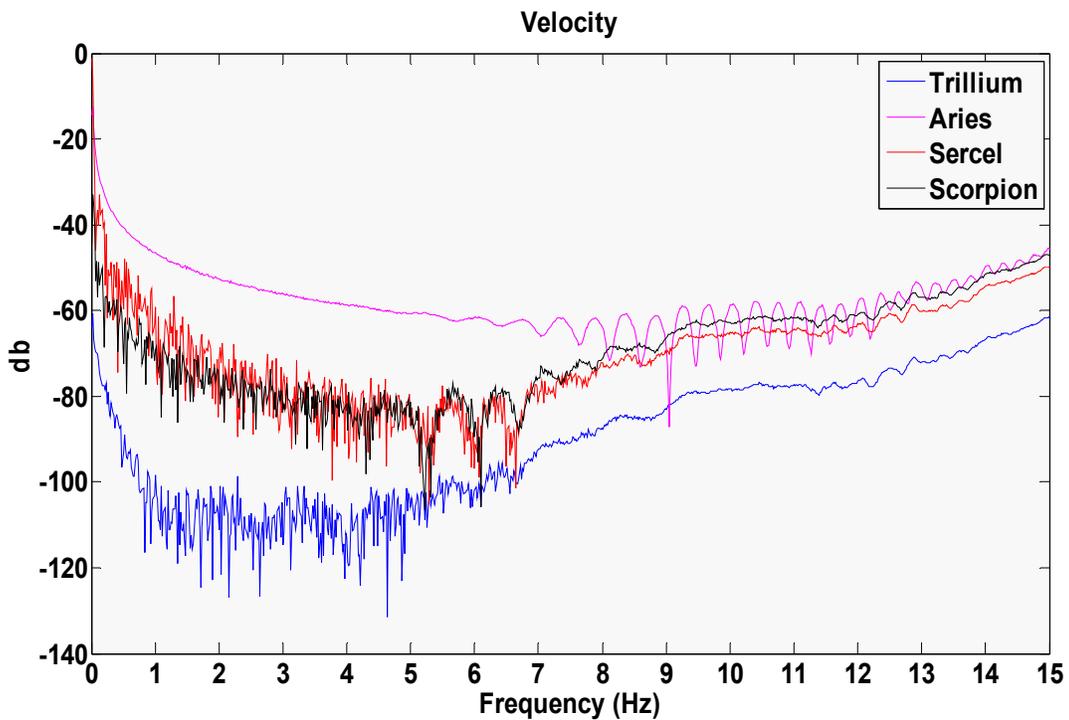

FIG. 5b. Visual comparison after converting raw data to velocity: data corrected for geophone and seismometer instrument response. (magnified portion of Figure 5a).
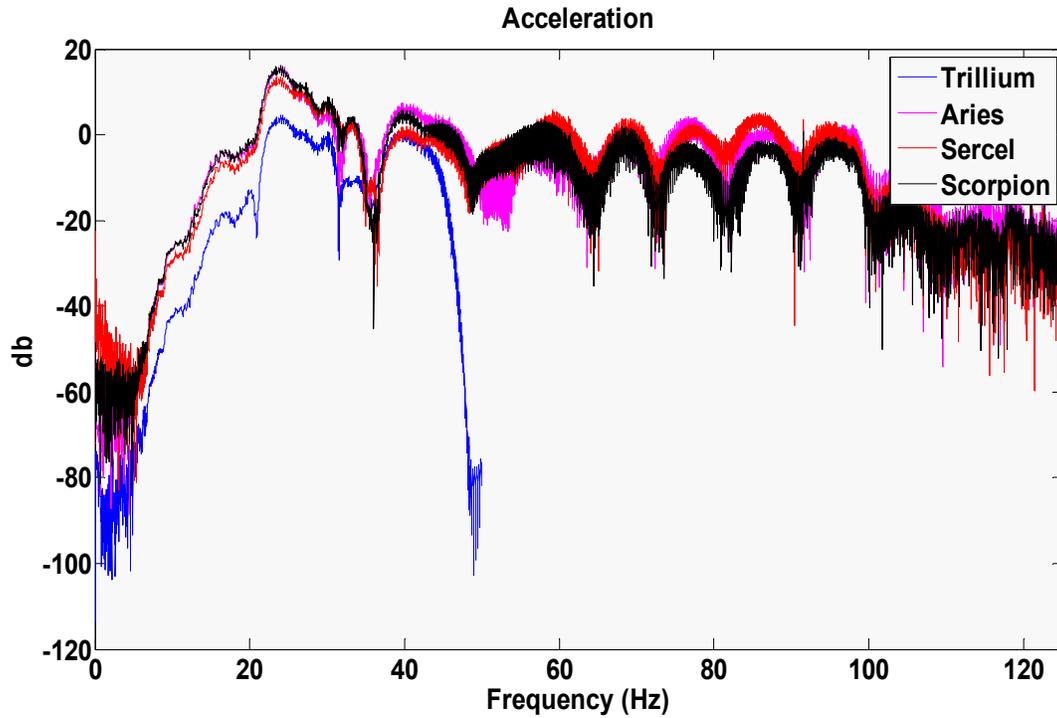
FIG. 6a. Visual comparison after converting raw data to acceleration: data corrected for geophone and seismometer instrument response.
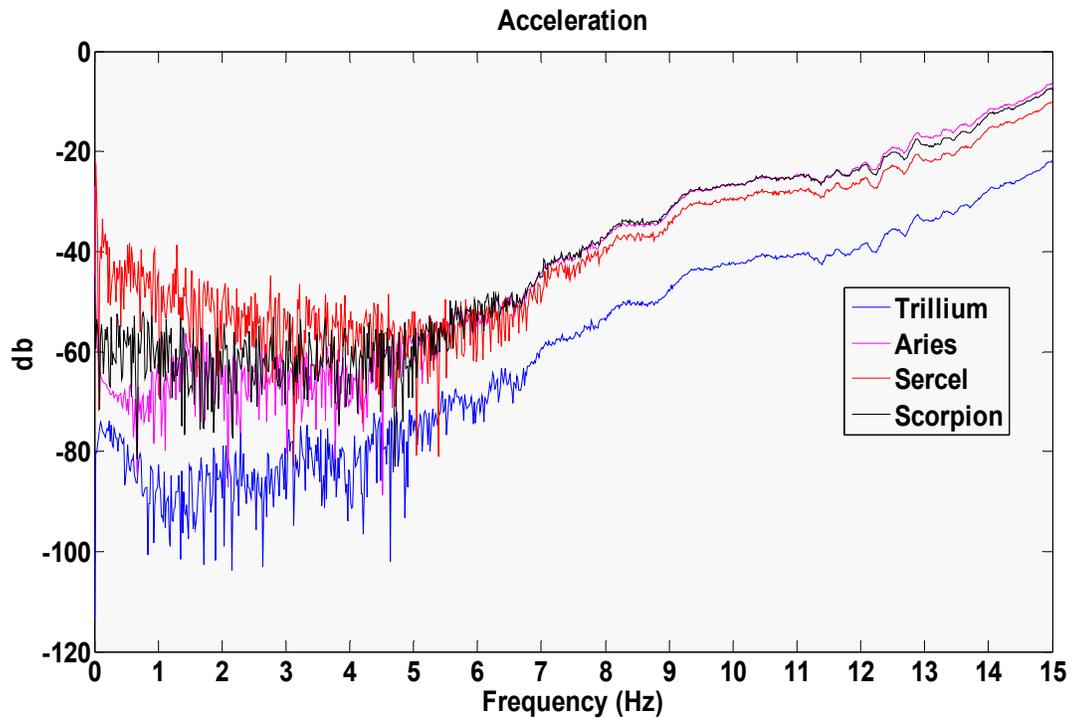

FIG. 6b. Visual comparison after converting raw data to acceleration: data corrected for geophone and seismometer instrument response. (magnified portion of Figure 3a).

Table 3. Least-squares-subtraction-scalar results. Values close to one are highlighted in red.

| Data	Trace1	Trace2	max(Trace1)	max(Trace2)	a [2:45 Hz]
raw	Aries	Trillium	1.12E-02	5.11E+05	9.18E-08
raw	Scorpion	Trillium	8.40E-03	5.11E+05	7.80E-08
raw	Sercel	Trillium	1.27E+05	5.11E+05	1.19E+00
velocity	Aries	Trillium	2.88E-04	3.55E-04	3.19E+00
velocity	Scorpion	Trillium	2.81E-04	3.55E-04	3.33E+00
velocity	Sercel	Trillium	2.13E-04	3.55E-04	2.59E+00
acceleration	Aries	Trillium	4.08E-02	3.52E-02	2.91E+00
acceleration	Scorpion	Trillium	4.13E-02	3.52E-02	2.98E+00
acceleration	Sercel	Trillium	3.17E-02	3.52E-02	2.31E+00
raw	Trillium	Aries	5.11E+05	1.12E-02	1.04E+07
raw	Scorpion	Aries	8.40E-03	1.12E-02	8.22E-01
raw	Sercel	Aries	1.27E+05	1.12E-02	1.24E+07
velocity	Trillium	Aries	3.55E-04	2.88E-04	2.94E-01
velocity	Scorpion	Aries	2.81E-04	2.88E-04	1.03E+00
velocity	Sercel	Aries	2.13E-04	2.88E-04	7.95E-01
acceleration	Trillium	Aries	3.52E-02	4.08E-02	3.18E-01
acceleration	Scorpion	Aries	4.13E-02	4.08E-02	1.03E+00
acceleration	Sercel	Aries	3.17E-02	4.08E-02	7.91E-01
raw	Aries	Sercel	1.12E-02	1.27E+05	7.49E-08
raw	Scorpion	Sercel	8.40E-03	1.27E+05	6.47E-08
raw	Trillium	Sercel	5.11E+05	1.27E+05	8.09E-01
velocity	Aries	Sercel	2.88E-04	2.81E-04	1.21E+00
velocity	Scorpion	Sercel	2.81E-04	2.81E-04	1.28E+00
velocity	Trillium	Sercel	3.55E-04	2.81E-04	3.61E-01
acceleration	Aries	Sercel	4.08E-02	3.17E-02	1.20E+00
acceleration	Scorpion	Sercel	4.13E-02	3.17E-02	1.27E+00
acceleration	Trillium	Sercel	3.52E-02	3.17E-02	3.82E-01
raw	Aries	Scorpion	1.12E-02	8.40E-03	1.17E+00
raw	Trillium	Scorpion	5.11E+05	8.40E-03	1.26E+07
raw	Sercel	Scorpion	1.27E+05	8.40E-03	1.53E+07
velocity	Aries	Scorpion	2.88E-04	2.81E-04	9.51E-01
velocity	Trillium	Scorpion	3.55E-04	2.81E-04	2.82E-01
velocity	Sercel	Scorpion	2.13E-04	2.81E-04	7.76E-01
acceleration	Aries	Scorpion	4.08E-02	4.13E-02	9.53E-01
acceleration	Trillium	Scorpion	4.13E-02	4.13E-02	3.03E-01
acceleration	Sercel	Scorpion	3.52E-02	4.13E-02	7.80E-01
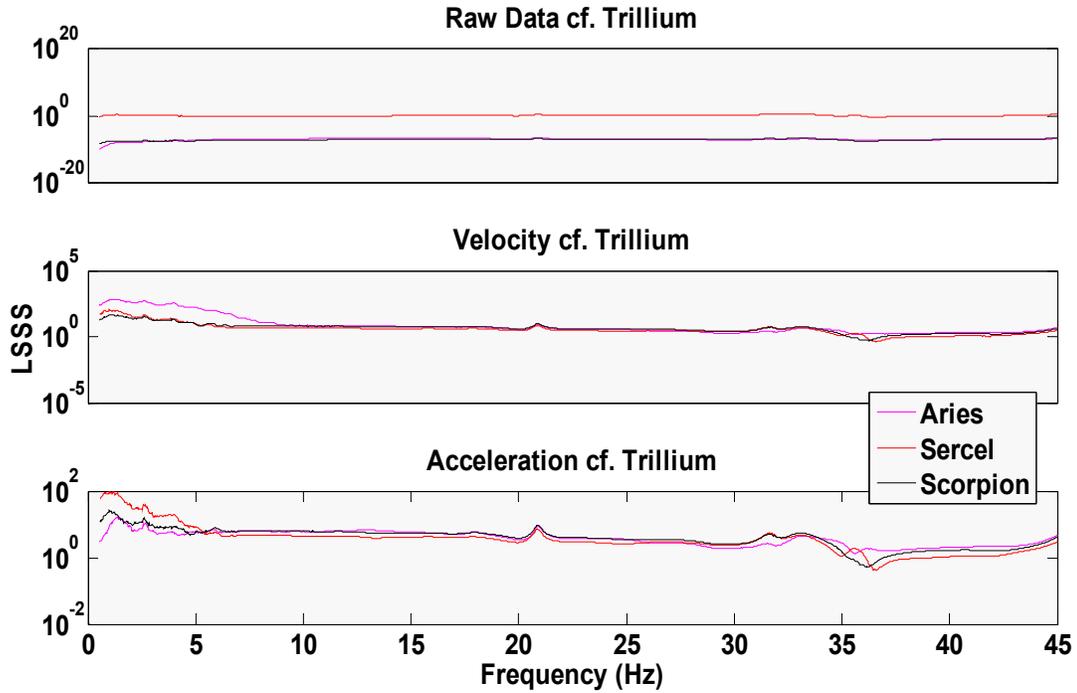
FIG. 7a. Frequency dependent Least-squares-subtraction-scalar curves for Figures 4-6: data compared to Trillium.
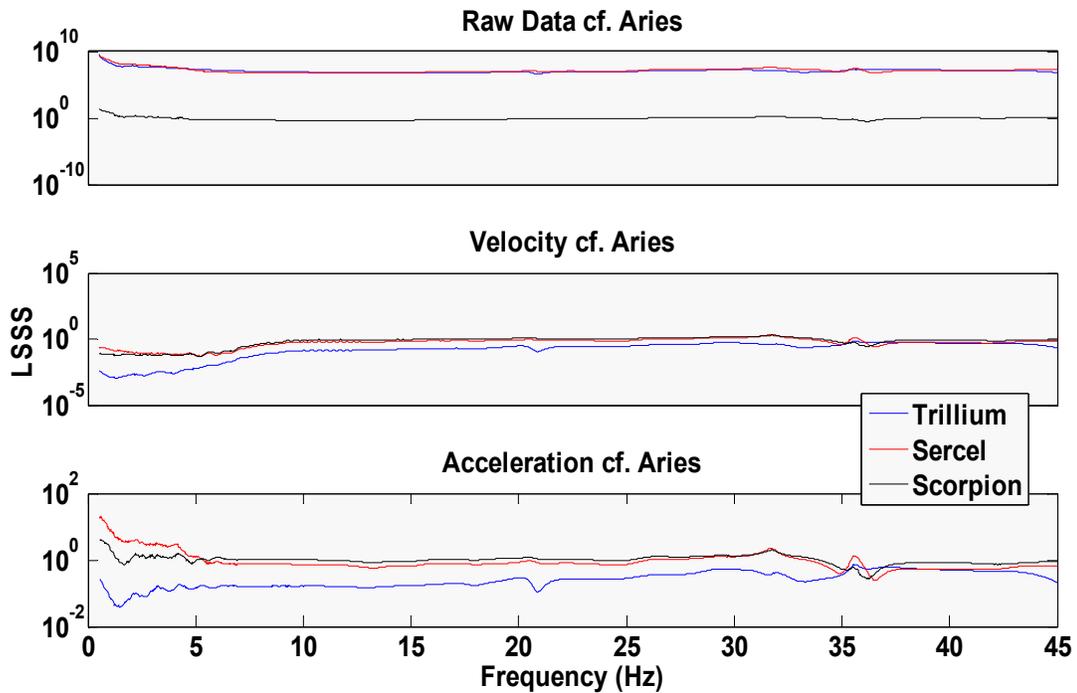

FIG. 7b. Frequency dependent Least-squares-subtraction-scalar curves for Figures 4-6: data compared to Aries.
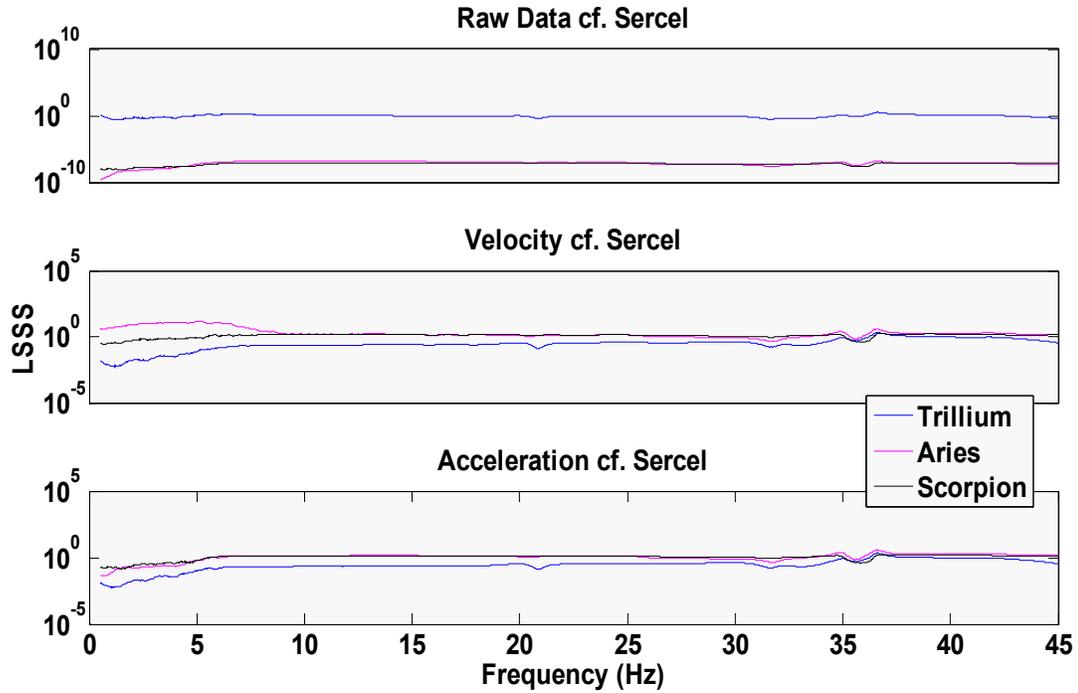
FIG. 7c. Frequency dependent Least-squares-subtraction-scalar curves for Figures 4-6: data compared to Sercel.
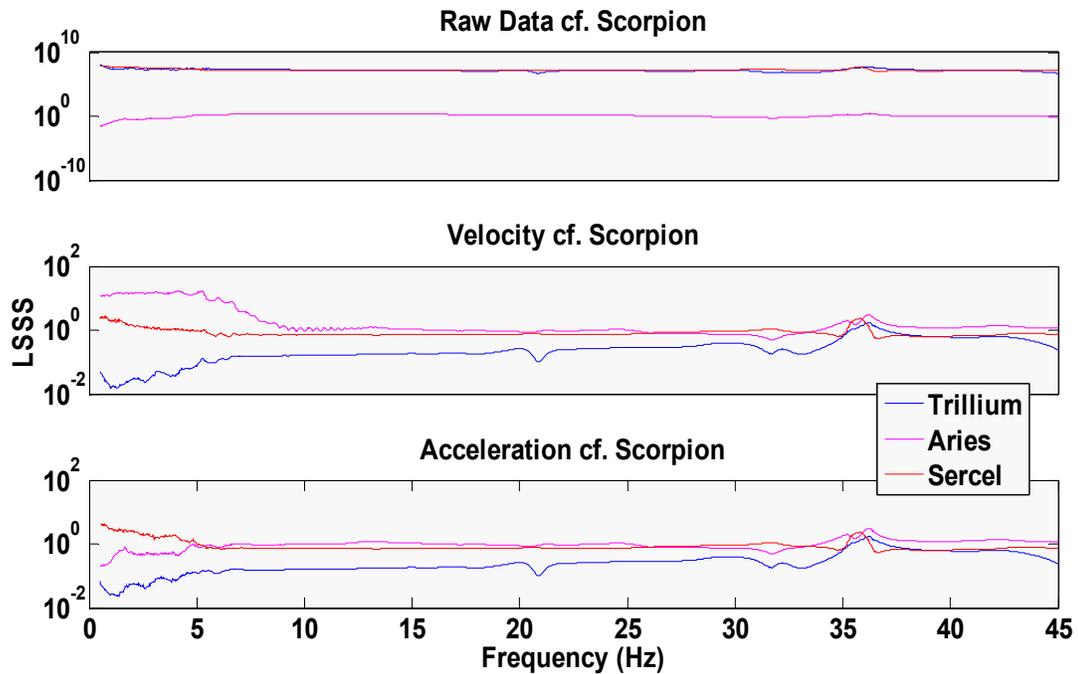

FIG. 7d. Frequency dependent Least-squares-subtraction-scalar curves for Figures 4-6: data compared to Scorpion.

DISCUSSION

Least-squares-subtraction scalars that are close to one in value are high-lighted in red in Table 3. The Sercel and Trillium uncorrected velocity and acceleration values are a close match, as are the Aries and Scorpion values. This can be taken to mean that the raw numbers in the SEG-Y file are the same order of magnitude. The Sercel, Scorpion and Aries comparisons are all close to one in the velocity and acceleration domains, but the comparisons to the Trillium data are ~three. This difference can be seen in Figures 4-6, where the Aries, Scorpion and Sercel data plot almost on top of each other, but the Trillium data are lower in amplitude, while having the same overall trend. This implies that there is a further factor of 3 that has not been accounted for in Equation(s) 1.

All data show notches at ~31.5 and ~35.5 Hz, but only the Trillium data has a notch at ~21 Hz (Figures 4a, 5a and 6a). All three notches clearly affect the least-squares results (Figure 7). Unexpectedly, the Aries geophone data compares best to the others in the acceleration domain (cf. Figures 5b and 6b).

System electrical noise appears to dominate signal below about 7 Hz for all systems, likely due to the low power used for the Vibrosies sweep, and the long start taper used for the low-frequency end of thesweep (< 10 Hz). That being said, we appear to have a close match (other than a multiplicative term) down to at least 5 Hz for all recording systems and sensors (eg. Figure 6b, Figure 7).

ACKNOWLEDGEMENTS

REFERENCES

Bertram, M.B., Hall, K.W., Margrave, G.F., Lawton, D.C., Wong, J., and Gallant, E.V, 2009, Seismic acquisition projects 2009, CREWES Research Report, 8, **21**.

Bogert, B.P., 1961. The transfer function of a short-period vertical seismograph: Bulletin of the Seismological Society of America, **51**.

Eaton, D.W., Pidlisecky, A., Ferguson, R.J., and Hall, K.W., 2009, Absolute strain determination from a calibrated seismic field experiment, CREWES Research Report, 17, **21**.

Hall, K.W., Margrave, G.F., and Bertram, M.B., 2009, Comparison of low-frequency data from co-located receivers using frequency dependent least-squares-subtraction scalars, CREWES Research Report, 27, **21**.

Hons, M.S., 2008, Seismic sensing: Comparison of geophones and accelerometers using laboratory and field data: M.Sc. Thesis. University of Calgary.

Nanometrics, 2008, Trillium 240 Seismometer User Guide: Part number 15672R4.

SM-24 geophone element brochure, 2006, http://www.geophone.com/techpapers/SM-24%20Brochure.pdf, accessed September, 2010.

Trillium 240 brochure, 2010, http://www.nanometrics.ca/index.php?option=com_content&view=article&id=22&Itemid=52, accessed September 2010.